ACS APPLIED MATERIALS & INTERFACES

Letter

www.acsami.org

Ultrasensitive Photodetectors Based on Island-Structured $CH_3NH_3PbI_3$ Thin Films

Yin Zhang,[†,‡,⊥] Juan Du,[†,‡] Xiaohan Wu,[‡] Guoqian Zhang,[‡] Yingli Chu,[‡] Dapeng Liu,[‡] Yixin Zhao,[*,§] Ziqi Liang,[*,∥] and Jia Huang[*,‡,⊥]

[‡]School of Materials and Engineering, Tongji University, Shanghai 201804, China

[⊥]Key Laboratory of Advanced Civil Engineering Materials, Tongji University, Ministry of Education, Shanghai 201804, China

[§]School of Environmental Science and Engineering, Shanghai Jiao Tong University, Shanghai 200240, China

[∥]Department of Materials Science, Fudan University, Shanghai 200433, China

Supporting Information

ABSTRACT: $CH_3NH_3PbI_3$ perovskite-based optoelectronics have attracted intense research interests recently because of their easy fabrication process and high power conversion efficiency. Herein, we report a novel photodetector based on unique $CH_3NH_3PbI_3$ perovskite films with island-structured morphology. The light-induced electronic properties of the photodetectors were investigated and compared to those devices based on conventional compact $CH_3NH_3PbI_3$ films. The island-structured $CH_3NH_3PbI_3$ photodetectors exhibited a rapid response speed (<50 ms), good stability at a temperature of up to 100 °C, a large photocurrent to dark current ratio ($I_{light}/I_{dark} > 1 \times 10^4$ under an incident light of ~6.59 mW/cm^2, and $I_{light}/I_{dark} > 1 \times 10^2$ under low incident light ~0.018 mW/cm^2), and excellent reproducibility. Especially, the performance of the island-structured devices markedly exceed that of the conventional compact $CH_3NH_3PbI_3$ thin-film devices. These excellent performances render the island-structured device to be potentially applicable for a wide range of optoelectronics.

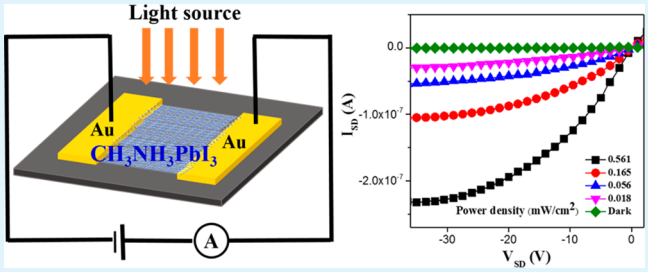

KEYWORDS: *photodetector, $CH_3NH_3PbI_3$ perovskites, high sensitivity, island-structured thin film, sensor*

Photodetectors can convert optical signals to electrical signals. They are essential elements applied in communications, environmental monitoring, optoelectronic circuits, and intelligent buildings.[1−3] In the past decade, extensive efforts have been devoted to explore the next generation photodetector materials, such as In_2Te_3, ZnO, and GaN, with low noise, high photosensitivity, and good stability. However, many of the reported photodetector materials still suffer from limited photocurrent and photoresponse speed.[4−6] Additionally, for a lot of practical applications, wide spectrum photodetection is necessary in order to improve the transmission rate and capacity. However, most of the studies on photodetectors or phototransistors mainly focused on light illumination under specific wavelength, because of the lack of proper materials that possess the ability to absorb incident radiation over a broad range of wavelength.[7−9] On the other hand, nanostructured and microstructured materials, such as nanowires and nanoparticles, have been demonstrated to show high photosensitivity, because their large surface-to-volume ratio can enhance the light scattering effect and light harvesting, and thus exhibit photodetection performance better than bulky counterparts. However, these nanostructured and microstructured devices usually need precise synthetic fabrication process using a combination of lithography, etching, and deposition, which is complicated, time-consuming, and uneconomic. Therefore, it is of great interest to develop new materials for high performance photodetectors by easy fabrication method.

Very recently, organolead halide perovskites, a new class of organic−inorganic hybrid materials, have attracted growing interests due to their easy fabrication and outstanding performances in photovoltaic devices and other optoelectronic devices.[10−13] As an ideal active material for optoelectronic devices, the band gap of organolead halide perovskite matches the energy of visible and near-IR light spectrum region. Additionally, organolead halide perovskites feature weakly bounded excitons with long lifetimes (~300 ns), which is also a significant advantage for applications in photodetector devices.[14,15] The production strategies of the hybrid perovskite thin film can be easily scaled and controlled. For example, Xie et al. and others had explored the photodetector applications based the $CH_3NH_3PbI_3$ thin film.[11,16−18] The high sensitivity and fast response of those devices demonstrate the promising advantages in applications. However, the photocurrent (on the order of nA) and the I_{light}/I_{dark} ratio (~300) of those devices could be further enhanced to extend the range of practical applications. Here in this work, we have significantly improved

Received: June 16, 2015
Accepted: September 21, 2015
Published: September 21, 2015

DOI: 10.1021/acsami.5b05221
ACS Appl. Mater. Interfaces 2015, 7, 21634−21638

photodetector performance by controlling $CH_3NH_3PbI_3$ film morphology through a simple and cost-effective solution method. The obtained $CH_3NH_3PbI_3$ films were composed of continuous micrometer-sized islands networks instead of a compact surface, exhibiting wide optical absorption over a broad range of wavelength. Due to the existence of islands network, the performance of device was significantly enhanced comparing to that of the conventional compact $CH_3NH_3PbI_3$ devices. The photocurrent can be generated and annihilated within 50 ms. Devices showed significantly higher photocurrent to dark current ratio ($I_{light}/I_{dark} > 1 \times 10^4$ at ~6.59 mW/cm^2) than that of previously reported devices.[11,16,20] A decent I_{light}/I_{dark} ratio ($>1 \times 10^2$) can still be achieved even when the device was only exposed to a light as weak as 0.018 mW/cm^2. Moreover, device stability was demonstrated at high temperature up to 100 °C.

The surface topography and cross section image of the island-structured $CH_3NH_3PbI_3$ film on a substrate is shown in Figure 1a, b. The surface of organolead halide perovskite films

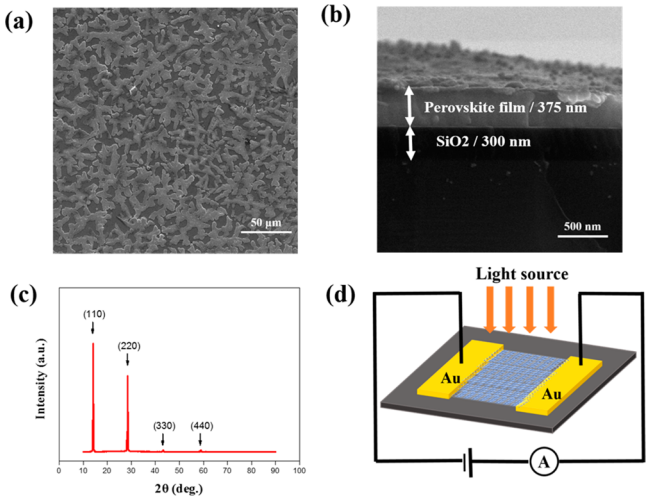

Figure 1. Scanning electron microscope (SEM) image of (a) $CH_3NH_3PbI_3$ perovskite thin film surface with island-structured morphology and (b) cross-sectional structure of the representative device. (c) XRD spectrum of the $CH_3NH_3PbI_3$ perovskite thin film on a glass substrate. (d) Schematic diagram of fabricated photodetector device components.

showed micrometer-sized islands forming random networks. The cross section image shows that the thickness of $CH_3NH_3PbI_3$ layer is about 375 nm. The result of Energy Dispersive Analysis System of X-ray (EDX) confirms the element ratio of $CH_3NH_3PbI_3$ (shown in Figure S1). No other foreign substances were presented. Figure 1c depicts the X-ray diffraction (XRD) spectrum of the prepared perovskite film spin-coated on a glass substrate. Four characteristic peaks centered at 14.16°, 28.50, 43.28, and 58.90° are assigned to the 110, 220, 330, and 440 planes of a tetragonal perovskite crystal structure with lattice parameter of a = 8.825 Å, b = 8.835 Å, c = 11.24 Å, which is consistent with literatures reported.[13,19] As shown in Figure S2, the strong and wide absorbance of the island-structured film demonstrates good light-harvesting capability over wavelength from 300 to 1000 nm range. Detailed device fabrication and measurement methods are introduced in the Supporting Information. Figure 1d shows a schematic diagram of the photodetector device structure. The $CH_3NH_3PbI_3$ film serves as the photosensitive material, and gold contacts act as electrodes to provide the bias voltage. A power-tunable white-light LED with wavelength ranging from 400 to 800 nm was used as the illumination source. The incident light power density was recorded using a commercial power meter (PM100D, Thorlabs). Electrical characterizations were recorded under different illumination power intensities. The measurements were carried out by sweeping the bias voltage between the two electrodes and tuning the illumination from dark to a given power density.

Figure 2a, b shows the photocurrent of the device as a function of bias voltages between two gold electrodes under

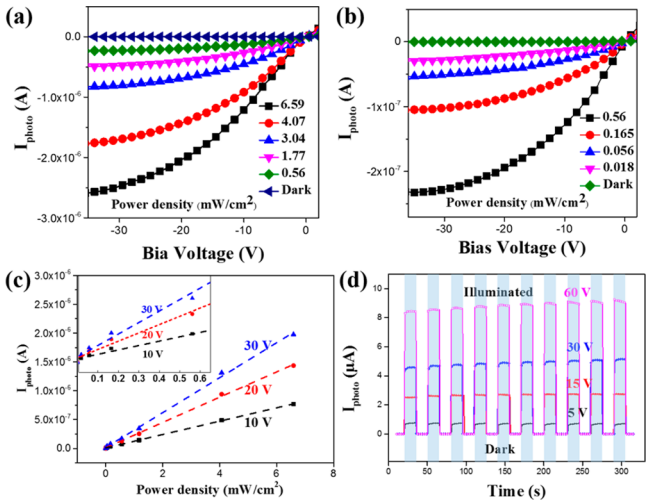

Figure 2. (a, b) $I-V$ characteristics of $CH_3NH_3PbI_3$ photodetectosr under different illumination power density. (c) Depencency of photocurrent on incident light power density and bias voltage; inset shows the magnification of the low power density region. (d) Transient photoresponse properties with bias voltage of 5, 15, 30, and 60 V under a power density of 6.59 mW/cm^2.

different incident light power densities. The photodetector current−voltage ($I-V$) characteristics were depicted both at low (0.018−0.561 mW/cm^2) and at high (0.56−6.59 mW/cm^2) light power densities range. The dark current of this photodetector at 30 V is ultralow (~1×10^{-10} A) in this case, After illuminating with a light power density of 6.59 mW/cm^2, the photocurrent increased by more than 10 000 times compared to that of the dark circumstance. Photodetectors usually have two modes: photoconductive mode and photovoltaic mode.[3] In our case, the device acts as an insulator under dark circumstance, and the photocurrent arises dramatically with the increase of light illumination, which exhibits as a typical photoconductive mode. Here, the photocurrent can be attributed to the electron−hole pairs generated by the incident phonons with energy equal or larger than the band gap. Compared with photodetectors based on conventional $CH_3NH_3PbI_3$ compact film, the island-structured thin films have a larger surface-to-volume ratio and thus contain more radiating area under similar illumination condition. As a result, the present photocurrent is significantly higher than that of devices with conventional $CH_3NH_3PbI_3$ compact film.[16,20]

The ultralow dark current suggests that the island-structured $CH_3NH_3PbI_3$ films are highly resistive in dark. Usually a low dark current is also essential to a high performance photodetectors device. The ultralow dark current of this photodetector may partially arise from the island-structured topography, because the physical boundaries among the

DOI: 10.1021/acsami.5b05221
ACS Appl. Mater. Interfaces 2015, 7, 21634−21638

$CH_3NH_3PbI_3$ islands can hinder charge transport. Because of the ultralow dark current, another remarkable feature of this device is the good photosensitivity to weak light illumination. As shown in Figure 2b, a decent I_{light}/I_{dark} ratio ($>1 \times 10^2$) can still be achieved even when the device was only exposed to a light as weak as 0.018 mW/cm^2. When a higher illumination intensity (~6.59 mW/cm^2) was used, devices showed significantly higher photocurrent to dark current ratio ($I_{light}/I_{dark} > 1 \times 10^4$) than that of most previously reported $CH_3NH_3PbI_3$ photodetectors to the best of our knowledge.[11,16,20]

The displayed high sensitivity to weak light illumination and large I_{light}/I_{dark} ratio of the presented photodetector is also better than a lot of nanomaterials-based device.[5,21,22] Such a drastic enhancement in these properties is very promising for practical applications such as photodiodes, current modification and signal magnification.[23−25]

The $I-V$ curves under light illumination show nonlinear dependence on the applied bias voltage, similar to field-effect transistors. From the $I-V$ curve in darkness (Figure S6a), we also observed the nonlinear and asymmetry characteristics at room temperature, confirming the existence of non-Ohmic contact. However, the $I-V$ curve in darkness is more linear at higher temperature, as shown in Figure S6b. It is possible that water and oxygen molecules were trapped in the active material at room temperature, which induce charge trapping effect and slightly shifted energy level of the active material. The mismatch between the energy level of $CH_3NH_3PbI_3$ active material and the Fermi level of gold electrode lead to the non-Ohmic contact. When the temperature increased, trapped molecules can be detrapped from the film and then the $I-V$ curve is more linear. In addition, the energy level of $CH_3NH_3PbI_3$ and the charge density is also the function of temperature. Increasing the temperature might reduce the energy level mismatch and thus lead to more linear $I-V$ curves. Because the dark current is very low (~1×10^{-10} A), signal noise can also contribute to the nonlinearity of the $I-V$ curves in darkness.

As plotted in Figure 2c, the photocurrent is linearly proportional to the incident irradiation intensity, with the fitted curve displaying different gradients corresponding to different applied voltages. Within the linear range, the islands-structured $CH_3NH_3PbI_3$ film acts as a typical photon-dependent detector. The current increases with the increasing of light power because the excited charge density increases with the increased photon number density. The linear dependence can be maintained in weak illumination range, as shown in the inset of Figure 2c. Moreover, this linear dependence can be maintained for different bias voltages. Similar to transistors using both gate voltages and a source−drain voltages to control the source−drain currents, in this case, the photodetectors can actually use both the incident light power densities and the applied bias voltages to modulate the photocurrents.

To further characterize the stability of the photocurrent response, we studied the transient photoresponse behavior of the devices with the illumination switched on and off at different bias voltages (5, 15, 30, and 60 V), as shown in Figure 2d. The duration of the on and off states was both sustained for 15 s. There is nearly no significant variation in the signal amplitude during the on/off cycles, indicating a good reversibility and stability of the device.

In addition to the intrinsic properties of $CH_3NH_3PbI_3$ perovskite materials, here the high I_{light}/I_{dark} ratio should also be attributed to the island networks morphology of $CH_3NH_3PbI_3$ film. The amounts of $CH_3NH_3PbCl_3$ used during fabrication was found to be critical for the resulting film morphology (see details in Materials and Methods in the Supporting Information). By using 1.5 and 0.75 mmol $CH_3NH_3PbCl_3$ in the precursor solutions, compact and island-structured $CH_3NH_3PbI_3$ films were obtained, respectively. As shown in Figure 3, the compact film has no islands

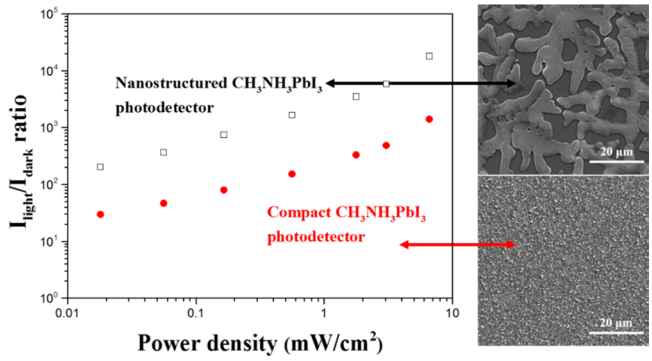

Figure 3. Comparison of I_{light}/I_{dark} ratio under various illumination power densities at a vias of 30 V between island-structured and compact $CH_3NH_3PbI_3$ photodetector, and their corresponding SEM images showing film morphology.

features because the increased amount of $CH_3NH_3PbCl_3$ could improve the crystallization of $CH_3NH_3PbI_3$ and lead to uniform films. It was reported that the compact $CH_3NH_3PbI_3$ significantly improved the power conversion efficiency of planar $CH_3NH_3PbI_3$ solar cells.[19] However, in the application of photodetector, as shown in Figure 3, the I_{light}/I_{dark} ratios of the device based on island structured $CH_3NH_3PbI_3$ are 1 order of magnitude higher than that of compact devices. The enhanced performance of island-structured $CH_3NH_3PbI_3$ might result both from the large surface-to-volume ratio and from the continuous island-structured networks. Large surface-to-volume ratio can enhance the light scattering effect and light harvesting of the active material. In addition, we believe that the charge transport in the island-structured perovskite films can be affected both by the semiconductor/metal interface, and by the interactions between neighboring islands due to the presence of boundaries. During charge transportation, the excited charges have to travel through these junction barriers among the micrometer-sized $CH_3NH_3PbI_3$ islands. Upon illumination, the increased charge density in each $CH_3NH_3PbI_3$ islands would lower the effective energy barrier height, which then allow easier charge tunneling and transportation than that of devices in darkness. This process results in a significant increase in the conductivity of the islands network. This mechanism, named "hopping-like" transportation, has also been successfully used to interpret the performance of other network-structured thin film device.[26−28] This interesting result helps to better understand the behavior of $CH_3NH_3PbI_3$ perovskite and other photosensitive materials.

Photoresponse speed is another key factor for photodetector. It determines the capability of a photodetector to follow a fast-varying optical signal. Here, promising device performance was also demonstrated by the fast response of our island-structured $CH_3NH_3PbI_3$ photodetector to light with a stepwise varying power density, as shown in Figure 4a. The time responses have been investigated at a bias 30 V, with light power densities of

DOI: 10.1021/acsami.5b05221
ACS Appl. Mater. Interfaces 2015, 7, 21634−21638

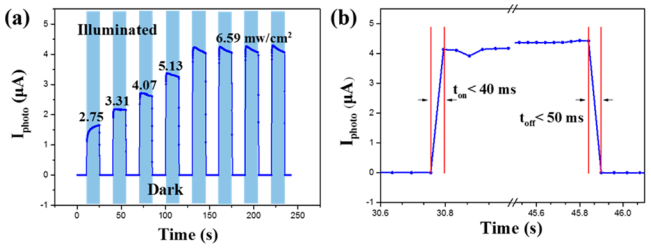

Figure 4. (a) Transient photoresponse characteristics of perovskite photodetector at different illumination power density. (b) Single photocurrent response cycle with light irradiation on and off, showing the response speed of the photodetector.

2.75, 3.31, 4.07, 5.13, and 6.59 mW/cm^2 being used. The light source was turned on and off for 15s each. Figure 4b shows that the device response time can be estimated from the enlarged portion of the plot containing one illumination on−off sequence. The response time, t_{on} and t_{off}, is defined as the photocurrent to increase from 10% to 90% of the peak value or vice versa, respectively. Both the response and recovery processes were completed rapidly, and the response time were less than 50 ms in both cases. It should be pointed out that the 50 ms response time was limited by our photocurrent measurement instrument. These observations indicate that the island-structured perovskite photodetectors have a rapid response time comparable to or faster than ZnO- and GaN-based semiconductor photodetectors.[1,2,29]

Such a fast response speed can also be attributed to the "hopping-like" charge transfer process. As previously discussed, the light illumination can increase excited charge density and then lower the energy barriers height between islands. When the light is turned off, the barrier height returns to its initial value in dark. The light-induced modulation of the barrier height between two adjacent $CH_3NH_3PbI_3$ islands should be a fast process upon varying the light, contributing to the fast response time of the device.[26,27]

In practical applications, the induced in situ heating, trapped electrons or contamination can cause device instability. In this concern, two series measurements were performed to study the stability of our device. First, we recorded the photocurrent for 150 s at various light power densities (6.59, 5.13, 4.07 mW/cm^2) with a bias voltage of 30 V. The result shows that the current maintains nearly stable without obvious decay, indicating excellent device stability (as shown in Figure S4). In addition, we measured the $I-V$ characteristics at various temperatures. As shown in Figure S5b, c, the $CH_3NH_3PbI_3$ based phototransistor works well at both 60 and 100 °C. The I_{light}/I_{dark} ratio could still achieve around 1×10^4 level at high temperature (100 °C).

In conclusion, island-structured $CH_3NH_3PbI_3$ perovskite films were developed by a simple solution-phase method and incorporated into photodetectors. The constructed devices showed high photosensitivity, excellent stability, high I_{light}/I_{dark} ratio, and rapid response speed. It is found that these excellent photodetector performances should be particularly attributed to the unique micrometer-sized islands networks morphology of organic−inorganic hybrid $CH_3NH_3PbI_3$. Compared to devices fabricated using compact $CH_3NH_3PbI_3$ films, the island-structured $CH_3NH_3PbI_3$ photodetector exhibited 1 order of magnitude higher photocurrent and I_{light}/I_{dark} ratio due to the presence of neighboring islands and the "hopping-like" charge transfer. The excellent performances and mechanism understanding open up possibilities of using island-structured hybrid perovskite for the next-generation photodetectors.

■ ASSOCIATED CONTENT

Supporting Information

The Supporting Information is available free of charge on the ACS Publications website at DOI: 10.1021/acsami.5b05221.

Materials and Methods, energy-dispersive analysis system of X-ray and UV−visible absorbance spectrum results, device I_{light}/I_{dark} ratio under different working voltage, device stability of long-term measurement, device temperature stability, $I-V$ curves in the darkness of the island-structured photodetector at various temperatures (PDF)

■ AUTHOR INFORMATION

Corresponding Authors

*E-mail: huangjia@tongji.edu.cn.
*E-mail: yixin.zhao@sjtu.edu.cn.
*E-mail: zqliang@fudan.edu.cn.

Author Contributions

†Y.Z. and J.D. contributed equally. The manuscript was written through contributions of all authors. All authors have given approval to the final version of the manuscript.

Funding

National Nature Science Foundation of China (Grants 51373123 and 21302142), Science & Technology Foundation of Shanghai (13PJ1408000 and 14JC1492600)

Notes

The authors declare no competing financial interest.

■ ACKNOWLEDGMENTS

The authors thank the characterization and testing center of school of materials and engineering at Tongji University. This work was supported by the National Nature Science Foundation of China (Grant Nos. 51373123 and 21302142), Science & Technology Foundation of Shanghai (13PJ1408000 and 14JC1492600), and the 1000 youth talent plan.

■ REFERENCES

(1) Liu, F.; Shimotani, H.; Shang, H.; Kanagasekaran, T.; Zólyomi, V.; Drummond, N.; Fal'ko, V. I.; Tanigaki, K. High-Sensitivity Photodetectors Based on Multilayer GaTe Flakes. *ACS Nano* **2013**, *8*, 752−760.

(2) Hatch, S. M.; Briscoe, J.; Dunn, S. A Self-Powered ZnO-Nanorod/CuSCN UV Photodetector Exhibiting Rapid Response. *Adv. Mater.* **2013**, *25*, 867−871.

(3) Wu, Y.; Yin, Z.; Xiao, J.; Liu, Y.; Wei, F.; Tan, K. J.; Kloc, C.; Huang, L.; Yan, Q.; Hu, F.; Zhang, H.; Zhang, Q. Crystal Structure and Phototransistor Behavior of N-Substituted Heptacence. *ACS Appl. Mater. Interfaces* **2012**, *4*, 1883−1886.

(4) Osinsky, A.; Gangopadhyay, S.; Gaska, R.; Williams, B.; Khan, M. A.; Kuksenkov, D.; Temkin, H. Low noise p-pi-n GaN Ultraviolet Photodetectors. *Appl. Phys. Lett.* **1997**, *71*, 2334−2336.

(5) Weng, W. Y.; Chang, S. J.; Hsu, C. L.; Hsueh, T. J. A ZnO-Nanowire Phototransistor Prepared on Glass Substrates. *ACS Appl. Mater. Interfaces* **2011**, *3*, 162−166.

(6) Wang, Z.; Safdar, M.; Jiang, C.; He, J. High-Performance UV−Visible−NIR Broad Spectral Photodetectors Based on One-Dimensional In2Te3 Nanostructures. *Nano Lett.* **2012**, *12*, 4715−4721.

(7) Xu, H.; Li, J.; Leung, B. H. K.; Poon, C. C. Y.; Ong, B. S.; Zhang, Y.; Zhao, N. A High-sensitivity Near-Infrared Phototransistor Based on an Organic Bulk Heterojunction. *Nanoscale* **2013**, *5*, 11850−11855.

DOI: 10.1021/acsami.5b05221
ACS Appl. Mater. Interfaces 2015, 7, 21634−21638

(8) Zhang, D.; Li, C.; Han, S.; Liu, X.; Tang, T.; Jin, W.; Zhou, C. Ultraviolet Photodetection Properties of Indium Oxide Nanowires. *Appl. Phys. A: Mater. Sci. Process.* **2003**, *77*, 163−166.
(9) Cheng, J.; Zhang, Y.; Guo, R. ZnO Microtube Ultraviolet Detectors. *J. Cryst. Growth* **2008**, *310*, 57−61.
(10) Schreier, M.; Curvat, L.; Giordano, F.; Steier, L.; Abate, A.; Zakeeruddin, S. M.; Luo, J. S.; Mayer, M. T.; Gratzel, M. Efficient Photosynthesis of Carbon Monoxide from CO2 Using Perovskite Photovoltaics. *Nat. Commun.* **2015**, *6*, 7326.
(11) Hu, X.; Zhang, X.; Liang, L.; Bao, J.; Li, S.; Yang, W.; Xie, Y. High-Performance Flexible Broadband Photodetector Based on Organolead Halide Perovskite. *Adv. Funct. Mater.* **2014**, *24*, 7373−7380.
(12) Sum, T. C.; Mathews, N. Advancements in Perovskite Solar Cells: Photophysics Behind The Photovoltaics. *Energy Environ. Sci.* **2014**, *7*, 2518−2534.
(13) Lee, M. M.; Teuscher, J.; Miyasaka, T.; Murakami, T. N.; Snaith, H. J. Efficient Hybrid Solar Cells Based on Meso-Superstructured Organometal Halide Perovskites. *Science* **2012**, *338*, 643−647.
(14) Wehrenfennig, C.; Eperon, G. E.; Johnston, M. B.; Snaith, H. J.; Herz, L. M. High Charge Carrier Mobilities and Lifetimes in Organolead Trihalide Perovskites. *Adv. Mater.* **2014**, *26*, 1584−1589.
(15) Marchioro, A.; Teuscher, J.; Friedrich, D.; Kunst, M.; van de Krol, R.; Moehl, T.; Gratzel, M.; Moser, J.-E. Unravelling the Mechanism of Photoinduced Charge Transfer Processes in Lead Iodide Perovskite Solar Cells. *Nat. Photonics* **2014**, *8*, 250−255.
(16) Xia, H.-R.; Li, J.; Sun, W.-T.; Peng, L.-M. Organohalide Lead Perovskite Based Photodetectors with Much Enhanced Performance. *Chem. Commun.* **2014**, *50*, 13695−13697.
(17) Li, D.; Dong, G. F.; Li, W. Z.; Wang, L. D. High Performance Organic-inorganic Perovskite-optocoupler Based on Low-Voltage and Fast Response Perovskite Compound Photodetector. *Sci. Rep.* **2015**, *5*, 6.
(18) Dou, L. T.; Yang, Y.; You, J. B.; Hong, Z. R.; Chang, W. H.; Li, G.; Yang, Y. Solution-processed Hybrid Perovskite Photodetectors with High Detectivity. *Nat. Commun.* **2014**, *5*, 6.
(19) Zhao, Y.; Zhu, K. CH3NH3Cl-Assisted One-Step Solution Growth of CH3NH3PbI3: Structure, Charge-Carrier Dynamics, and Photovoltaic Properties of Perovskite Solar Cells. *J. Phys. Chem. C* **2014**, *118*, 9412−9418.
(20) Guo, Y. L.; Liu, C.; Tanaka, H.; Nakamura, E. Air-Stable and Solution-Processable Perovskite Photodetectors for Solar-Blind UV and Visible Light. *J. Phys. Chem. Lett.* **2015**, *6*, 535−539.
(21) Zhai, T.; Fang, X.; Liao, M.; Xu, X.; Zeng, H.; Yoshio, B.; Golberg, D. A Comprehensive Review of One-Dimensional Metal-Oxide Nanostructure Photodetectors. *Sensors* **2009**, *9*, 6504−6529.
(22) Lu, J.; Sun, C.; Zheng, M.; Wang, Y.; Nripan, M.; van Kan, J. A.; Mhaisalkar, S. G.; Sow, C. H. Ultrasensitive Phototransistor Based on K-Enriched MoO3 Single Nanowires. *J. Phys. Chem. C* **2012**, *116*, 22015−22020.
(23) Asif Khan, M.; Kuznia, J. N.; Bhattarai, A. R.; Olson, D. T. Metal Semiconductor Field Effect Transistor Based on Single Crystal GaN. *Appl. Phys. Lett.* **1993**, *62*, 1786−1787.
(24) Mihailetchi, V.; Wildeman, J.; Blom, P. Space-Charge Limited Photocurrent. *Phys. Rev. Lett.* **2005**, *94*, 126602.
(25) Lee, Y.; Kwon, J.; Hwang, E.; Ra, C. H.; Yoo, W. J.; Ahn, J. H.; Park, J. H.; Cho, J. H. High-Performance Perovskite-Graphene Hybrid Photodetector. *Adv. Mater.* **2015**, *27*, 41−46.
(26) Chen, M.; Hu, L. F.; Xu, J. X.; Liao, M. Y.; Wu, L. M.; Fang, X. S. ZnO Hollow-Sphere Nanofilm-Based High-Performance and Low-Cost Photodetector. *Small* **2011**, *7*, 2449−2453.
(27) Yan, C. Y.; Singh, N.; Lee, P. S. Wide-bandgap Zn2GeO4 Nanowire Networks as Efficient Ultraviolet Photodetectors with Fast Response and Recovery Time. *Appl. Phys. Lett.* **2010**, *96*, 3.
(28) Hu, L. F.; Wu, L. M.; Liao, M. Y.; Fang, X. S. High-Performance NiCo2O4 Nanofilm Photodetectors Fabricated by an Interfacial Self-Assembly Strategy. *Adv. Mater.* **2011**, *23*, 1988−1992.
(29) Chiou, Y. Z.; Su, Y. K.; Chang, S. J.; Chen, J. F.; Chang, C. S.; Liu, S. H.; Lin, Y. C.; Chen, C. H. Transparent TiN Electrodes in GaN Metal-Semiconductor-Metal Ultraviolet Photodetectors. *Jpn. J. Appl. Phys.* **2002**, *41*, 3643−3645.

DOI: 10.1021/acsami.5b05221
ACS Appl. Mater. Interfaces 2015, 7, 21634−21638